

Supplemental Document

# Efficient Third Harmonic Generation from magnetic resonance in Low-index Dielectric Nanopillars

Rui Xie <sup>1</sup>, Xiaobo He <sup>2</sup>, Wenqiang Wang <sup>3</sup>, Liren Zheng <sup>1,\*</sup> and Junjun Shi <sup>1,4,\*</sup>

<sup>1</sup> Shandong Provincial Engineering and Technical Center of Light Manipulation and Shandong Provincial Key Laboratory of Optics and Photonic Devices, School of Physics and Electronics, Shandong Normal University, Jinan 250014, China.

<sup>2</sup> Institute of Physics, Henan Academy of Sciences, Zhengzhou, China.

<sup>3</sup> School of Physics and Technology, Wuhan University, Wuhan 430072, China.

<sup>4</sup> Henan Key Laboratory of Quantum Materials and Quantum Energy, School of Quantum Information Future Technology, Henan University

## Contents:

**S1: Influence from polymer with different refractive index.**

**S2: Influence on the reflection spectra from the size of the covered Au disk.**

**S3: The resonance condition for the Au/polymer/Au film.**

**S4: Influence on the reflection spectra from polymer pillar radius.**

**S5: Comparisons of the THG conversion efficiency**

**S6: THG conversion efficiency versus different pump light pulse duration.**

### S1: Influence from polymer with different refractive index.

Figure S1 presents the enhanced factor spectra with different polymer. The refractive index of dielectric is increased from 1.2 to 1.8 with the step 0.1. The sensing capabilities has the sensitivity

$$S = \frac{\Delta\lambda}{\Delta n} = 560 \text{ nm} \text{ and figure of merit FOM} = 47, \text{ which shows the sensing potential.}$$

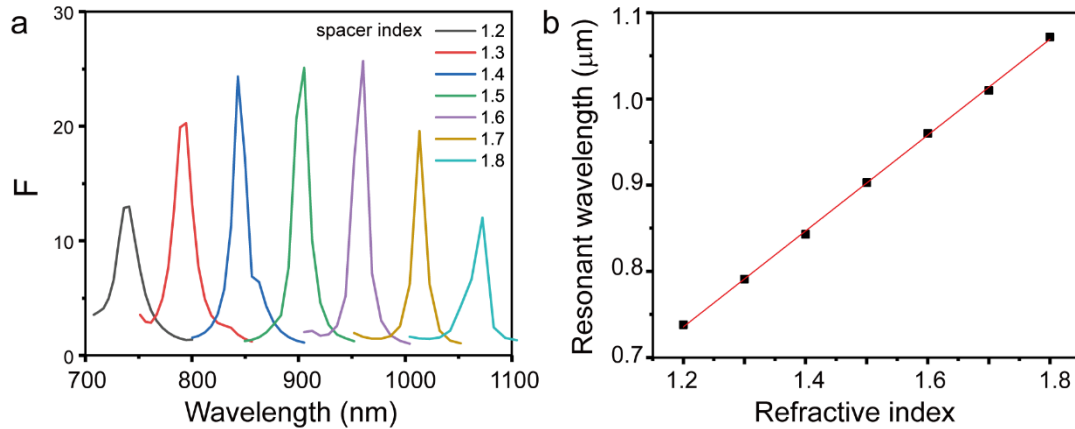


Figure S1. (a) The enhance factor (F) with different polymer. (b) The relationship between refractive index and resonant wavelength.

### S2: Influence on the reflection spectra from the size of the covered Au disk.

The upper covered Au disk provides the high reflection boundary which will benefit the improvement of the light power energy confined in the polymer pillars. Figure S2a shows that the thickness of the Au disk larger than 40 nm will show the higher-Q resonance than thinner covering. In Figure S2b, the radius of the pillar is fixed at 400 nm.

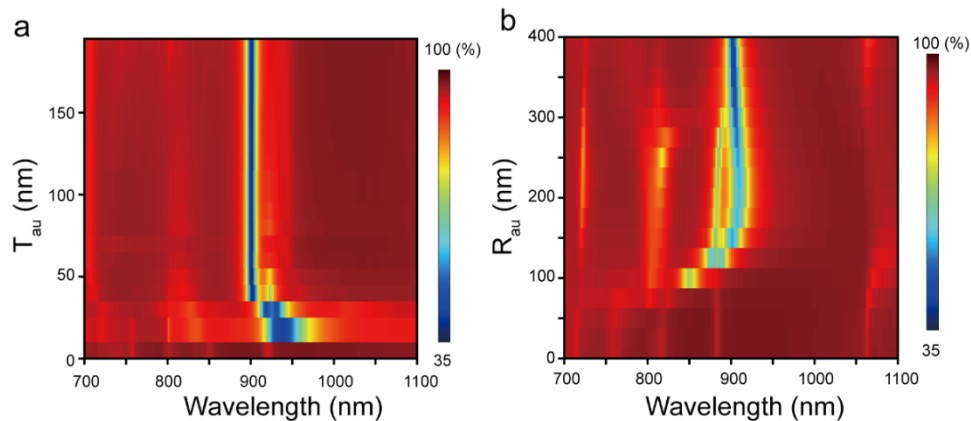


Figure S2. Influence on the reflection spectra from the size of the covered Au disk.

### S3: The resonance condition for the Au/polymer/Au film.

Figure S3 shows the dependence of the total energy stored in the polymer spacer on the spacer thickness and incident wavelength at the fundamental frequency. The dashed white lines show the different order of FP resonance where the thickness fits  $m/3$  wavelengths into the cavity formed by the sandwiched film. The resonance condition agrees well with the Fabry-Pérot resonance condition.

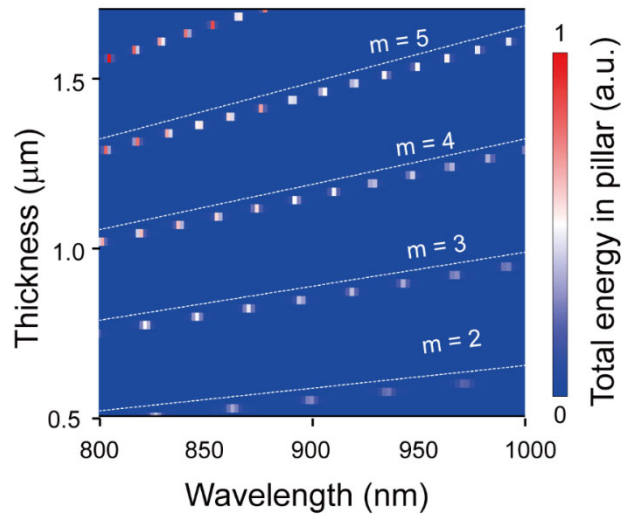


Figure S3. Resonance condition for Au/polymer/Au film.

### S4: Influence on the reflection spectra from polymer pillar radius.

Figure S4 shows the dependence of the reflection spectra between the pillar radius and the wavelengths. The radius of the covered Au disk is equal to that of the pillar. The resonant wavelength is red-shifted when the pillar radius is getting larger.

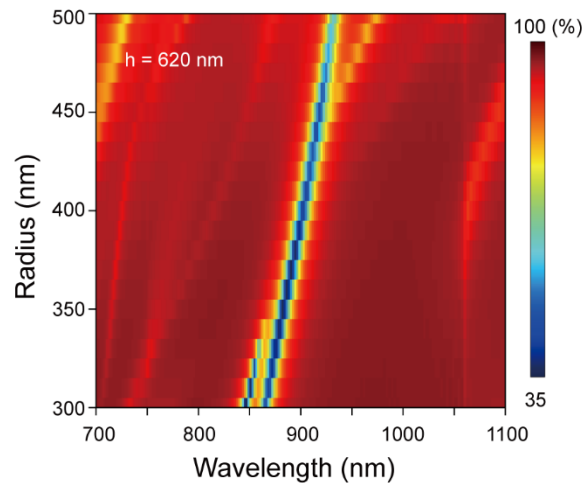


Figure S4. Influence on the reflection spectra from polymer pillar radius.

### S5: Comparisons of the THG conversion efficiency

Table 1 shows the comparisons of the THG conversion efficiency of different structures where the proposed nanostructure in this article appears in bold. The THG conversion efficiency is high up to the order of  $\sim 10^{-6}$ , which is higher than the case of some other configurations such as nanoantennas and metasurfaces. The proposed nano-structure is well made and yield higher conversion efficiency through MD enhancement might find applications in such as nanophotonics and biophotonics.

**Table S1 Comparisons of THG conversion efficiency of different structures.**

Structure	Structure parameter (diameter D, height h)	FF power or peak intensity ( $\lambda_{FW}$ )	THG efficiency	references
Ge nanodisk	D = 875 nm, H = 100nm	1 $\mu$ W, 5 GW/cm <sup>2</sup> peak intensity (1650nm)	0.0001%	Nano Lett. 2016, 16, 4635-4640.
Si nanodisk	D = 360 nm, H = 260 nm,	30m W, 5.5 GW/cm <sup>2</sup> peak intensity (1260nm)	10 <sup>-7</sup>	Nano Lett. 2014, 14, 6488-6492
Si metasurface	p=916.67 nm h=590 nm dx=740 nm dy=550 nm	1.2 GW/cm <sup>2</sup> (1560 nm)	2.8 $\times 10^{-7}$	Light Sci Appl. 12, 97 (2023)
TiO <sub>2</sub> metasurface	d = 272 nm, p = 332 nm, h = 150 nm	1.4 mW, 8.9 GW/cm <sup>2</sup> (555 nm)	2 $\times 10^{-7}$	Nano Lett. 2019, 19, 8972-8978.
Au/polymer/Au	D = 800 nm H <sub>polymer</sub> = 620 nm H <sub>au</sub> = 50 nm	0.01 GW/cm <sup>2</sup> (900 nm)	3 $\times 10^{-6}$	<b>This work</b>

### S6: THG conversion efficiency versus different pump light pulse duration.

In Figure S5, it is evident that the optimal pulse duration lies at approximately 90 fs, leading to a THG conversion efficiency of up to  $3 \times 10^{-6}$ . Beyond this duration, the THG conversion efficiency plateaus and gradually approaches saturation, which is a typical characteristic of cavity phenomena.

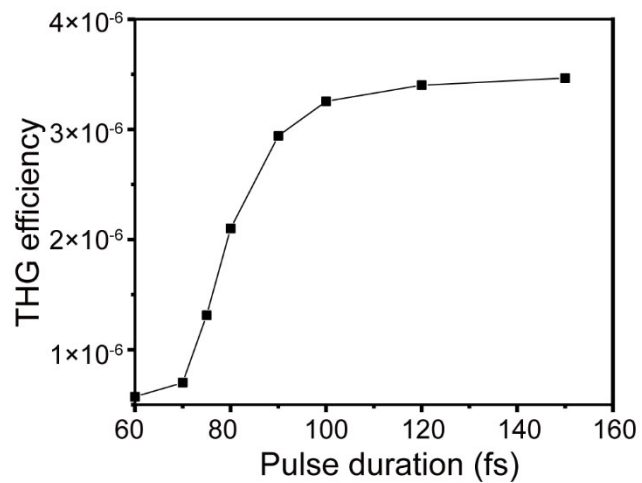


Figure S5. THG conversion efficiency versus different pump light pulse duration.